CRYSTAL GROWTH & DESIGN

Article

pubs.acs.org/crystal

Attachment and Detachment Processes of Individual Lysozyme Molecules on a Surface of a Monoclinic Lysozyme Crystal Studied by Fluorescent Single-Molecule Visualization

Guoliang Dai,[†,‡] Lei Zheng,[⊥] Gen Sazaki,*[,‡] and Yoshinori Furukawa[‡]

[†]Key Laboratory of Microgravity (National Microgravity Laboratory), Institute of Mechanics, Chinese Academy of Sciences, No. 15 Beisihuanxi Road, Beijing 100190, China

[‡]Institute of Low Temperature Science, Hokkaido University, N19-W8, Kita-ku, Sapporo 060-0819, Japan

[⊥]School of Civil Engineering, Southeast University, China, No. 2 Si Pai Lou, Nanjing, Jiangsu 210096, China

Supporting Information

ABSTRACT: On a $\{10\bar{1}\}$ face of a monoclinic crystal of hen egg-white lysozyme (HEWL), we visualized the attachment and detachment processes of individual fluorescent-labeled HEWL (F-HEWL) molecules by a fluorescent single-molecule visualization technique. We measured the changes in number density of F-HEWL molecules, whose positions were not changed for longer than a certain residence time, as a function of an adsorption time. We first confirmed that under an equilibrium condition, there was an "induction period" (~120 min) of the attachment/detachment processes, during which period the number density remained constant. After the induction period, the number density increased linearly with the adsorption time, as it was recently found on a tetragonal HEWL crystal [Dai, G. L. *Cryst. Growth Des* **2011**, *11*(1), 88−92]. In addition, we performed similar measurements under a supersaturated condition. Then we found that supersaturation significantly enhanced the attachment process after the induction time. The attachment/detachment processes finally reached a steady state, in which the attachment rate was higher than the detachment one. Moreover, we also found that in a rare case, an F-HEWL molecule adsorbed on a step laterally moved following the advancement of a growing step.

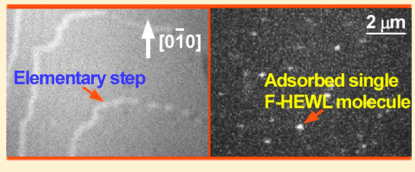

1. INTRODUCTION

During crystal growth, attachment/detachment processes of solute molecules on a crystal surface are key elementary processes that are still unclear. To reveal how the dynamics of attachment/detachment processes affects the crystallization process, one should know the behavior of individual molecules. Ensemble averaging approaches, such as spectroscopy and quartz crystal microbalance, usually need relatively large amount of molecules, and information cannot be obtained on the locations and attachment/detachment events of individual molecules. Hence, ensemble averaging approaches are less promising for investigating the attachment/detachment processes during crystal growth.

A single-molecule technique is a powerful way to study the behavior of individual molecules, avoiding ensemble averaging.[1] Therefore, from the end of the last century, the single-molecule technique, in particular, atomic force microscopy (AFM), was applied in the studies of attachment/detachment processes on a crystal surface; e.g., Vekilov and co-workers directly observed the near-critical-size clusters formed during the crystallization of apoferritin (protein) by AFM and analyzed the number of attached and detached molecules/aggregates.[2] However, Van Driessche and co-workers recently revealed that the scan of a cantilever of AFM significantly enhances the mass transfer of solute to a crystal surface.[3] AFM also cannot be applied to quick attachment/detachment events on a wide crystal surface because of its slow response. Hence, the attachment/detachment processes should be studied by fully noninvasive and quick-response techniques other than AFM.

One such promising technique is total internal reflection fluorescence (TIRF) microscopy, by which one can track individual fluorescent molecules at a submicron size scale.[4−8] Recently, one of the authors (G.S.) applied TIRF microscopy to the study on the diffusion of individual hen egg-white lysozyme (HEWL) molecules on the interface between a tetragonal HEWL crystal and an equilibrium HEWL solution.[9] Sazaki et al. demonstrated that TIRF microscopy can be a powerful tool to directly and noninvasively visualize the dynamic behavior of individual protein molecules on an interface between a protein crystal and a protein solution. Van Dreassche et al. also revealed the relation between adsorption sites of impurities and their effects on step advancement by TIRF microscopy.[10]

To our knowledge, we performed the first direct visualization of the attachment/detachment processes of fluorescent-labeled HEWL (F-HEWL) molecules on a relatively large interface (50 × 50 μm^2) between a tetragonal HEWL crystal (several hundred micrometers in thickness) and an equilibrium HEWL solution.[11] We revealed an induction period (~70 min) after which the number density of F-HEWL molecules adsorbed

Received: July 25, 2014
Revised: August 22, 2014
Published: August 29, 2014

mainly on steps increased linearly with the adsorption time. We showed the direct evidence that the residence time of molecules on the crystal surface gradually increases during the transition process from a solute species to the crystal after successive multistep processes. However, in our previous study,[9,11] we observed that F-HEWL molecules existed in a solution layer of 1 μm thickness between a crystal surface and a glass plate because of optical requirements (see Supporting Information Figure S1). Hence, we could not observe F-HEWL molecules in a supersaturated solution because of the depletion of solute in the 1-μm-thick solution layer (also see Figure S1).

In this study, we used a monoclinic HEWL crystal instead of a tetragonal one. Since a monoclinic HEWL crystal exhibits a thin-plate-like shape and has a thickness of only ~15 μm (distance between two opposed $\{10\bar{1}\}$ faces), we can perform TIRF microscopy observation on an interface between a crystal and a "free bulk HEWL solution" (also see Figure S1). Hence, under an equilibrium condition, we first tried to confirm whether the phenomena found in our previous study[11] using a tetragonal crystal and a thin solution layer can be general phenomena. Then next we tried to carry out similar observations under a supersaturated condition and tried to explore how supersaturation affects the attachment/detachment processes of individual molecules during the growth of a crystal.

2. EXPERIMENTAL SECTION

HEWL of 99.99% purity was purchased from Maruwa Food Industries, Inc., Japan (discontinued). To prepare F-HEWL, only the ε-amino group of the N-terminal of HEWL was specifically labeled with a fluorescent label, tetramethylrhodamin-5-isotiocyanate, according to the recipe of Matsui et al.[12]

Molecular weight of the fluorescent label is smaller than 3% of that of a HEWL molecule. In addition, most of the surface of an F-HEWL molecule is the same as that of a native HEWL molecule. Hence, the fluorescent label does not affect the translational/rotational diffusion and adsorption processes on a HEWL crystal surface. Therefore, during these processes, F-HEWL molecules can mimic native solute HEWL molecules. However, once F-HEWL molecules are incorporated into steps (more precisely kinks on steps), the fluorescent label prevents the subsequent formation of proper intermolecular bonding. Hence, after the incorporation into steps, F-HEWL molecules work as an impurity.[12]

Monoclinic HEWL seed crystals were grown by a batch method.[13] Then they were transferred into an observation chamber and placed on a bottom surface, as shown schematically in Figure 1. The

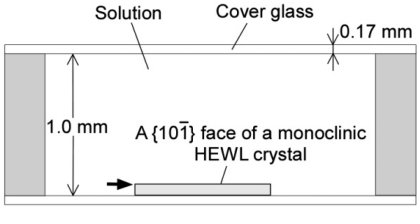

Figure 1. A sectional view of an observation chamber. The black bold arrow shows the observed interface between a monoclinic HEWL crystal and a bulk HEWL solution.

temperature inside the chamber was controlled at 20.0 ± 0.1 °C, using Peltier elements. The solution in the chamber contained 0.1 nM F-HEWL, 20 mg/mL $NaNO_3$, 50 mM sodium acetate (pH 4.5), and HEWL of two different concentrations. The concentrations C of HEWL solutions used to obtain an equilibrium condition and a growth condition were 1.1 and 1.55 mg/mL, respectively (solubility C_e is 1.1 mg/mL under our experimental conditions[13]). The absence of aggregates of F-HEWL molecules in the solution was confirmed by native-polyacrylamide gel electrophoresis. No deoxidation reagent, which is useful to prolong the fluorescence lifetime before photobleaching occurs, was used to avoid any deleterious effects on HEWL crystals.

A TIRF microscopy system using an objective was constructed on an inverted fluorescence microscope (IX70, Olympus) equipped with a 60× oil-immersion objective (PlanApo 60x TIRFM3, Olympus). Other details were explained in our previous study.[9,11] The focus of the objective was set at the interface marked by the bold arrow (Figure 1). F-HEWL molecules were illuminated with a 532 nm laser (fluence 0.11 kW/cm^2), and emission at ≥580 nm from F-HEWL was recorded using a dichroic mirror and an electron-multiplying charge-coupled device camera (EM-CCD; DV887; Andor Technology). The frame rate of the EM-CCD camera was set at 0.1 s, which is the lower limit for the detection of single F-HEWL molecules under our experimental conditions. To avoid photobleaching of F-HEWL, an electromagnetic shutter of the laser was sequentially opened and closed, as shown schematically in Figure 2a,b (respectively under the equilibrium and growth conditions). Since the average lifetime for photobleaching was ~40 s under our experimental conditions, the fluorescent observation was stopped within 23 s (Figure 2a) and 11 s (Figure 2b) of total irradiation, respectively. Individual F-HEWL molecules were successfully observed in situ, and one bright dot corresponds to one F-HEWL molecule (see Figure 3b).

Monoclinic HEWL crystals are usually grown by the spiral growth mechanism under our experimental conditions.[13] Distance between adjacent spiral steps in the $[0\bar{1}0]$ direction (2−3 μm) is much longer than that in the perpendicular direction (0.5−1 μm) (see Figure 8). Hence, all observations were carried out on spiral growth hillocks toward the $[0\bar{1}0]$ direction.

Before and after the single-molecule visualization, the surface morphology of a monoclinic HEWL crystal (Figure 3a) was observed by laser confocal microscopy combined with differential interference contrast microscopy (LCM-DIM), by which at first elementary steps on protein crystal surfaces (several nanometers in height)[14] and later elementary steps on ice crystal surfaces (0.37 nm in height)[15] can be visualized with sufficient contrast. From the in situ observation of elementary steps on a monoclinic HEWL crystal by LCM-DIM, we confirmed that elementary steps were not proceeding or receding, proving that a crystal had been maintained in the equilibrium condition during the single-molecule visualization. From the surface morphology image (Figure 3a) and single-molecule visualization image (Figure 3b), we also found the positions of F-HEWL molecules adsorbed on a crystal surface, as shown in Figure 3c (a composite image). Dust particles (marked by rectangles) worked as good markers to ensure the observation of the same field of view.

3. RESULTS AND DISCUSSION

3.1. Under an Equilibrium Condition. At an interface between a monoclinic HEWL crystal and an equilibrium bulk solution, we could visualize individual F-HEWL molecules. As shown in Figure 3c, on a $\{10\bar{1}\}$ face of a monoclinic HEWL crystal, F-HEWL molecules appeared to adsorb on both steps and terraces, although F-HEWL molecules mainly adsorbed on steps on a {110} face of a tetragonal HEWL crystal.[11] With respect to this difference, at present, we have no explanation based on intermolecular interaction. In the next section, we will discuss an F-HEWL molecule adsorbed on an elementary step growing in the lateral direction.

Figure 4 shows a typical example of the temporal change in the adsorbed F-HEWL molecules on a monoclinic HEWL crystal. In Figure 4a, white circles show all F-HEWL molecules visualized at the interface. In Figure 4b, red circles correspond to the molecules that were visualized at the same position 1 s after Figure 4a was taken. As explained in our previous study,[11] we can prove that the molecules visualized at the same positions (red circles) were not the case in which the molecules

dx.doi.org/10.1021/cg501122f | Cryst. Growth Des. 2014, 14, 5303−5309

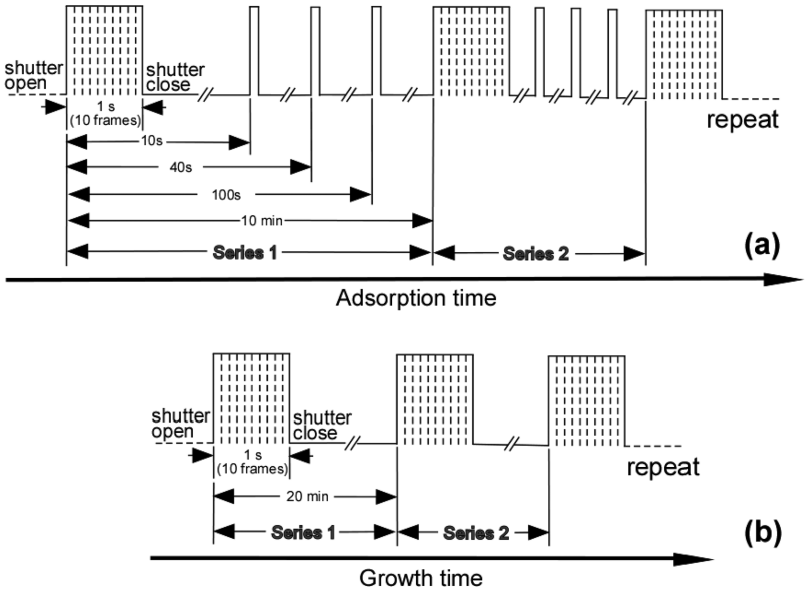

Figure 2. A time-sequence diagrams of the pulsed discontinuous laser illumination. (a) Under an equilibrium condition. (b) Under a supersaturated (growth) condition. Total irradiation periods for the fluorescent observations were 23 s (a) and 11 s (b), respectively. The average lifetime of F-HEWL for photobleaching was ~40 s under our experimental conditions.

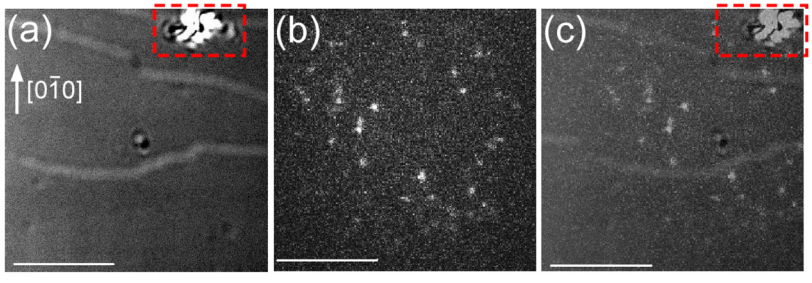

Figure 3. Elementary steps and F-HEWL molecules on a {10$\bar{1}$} face of a monoclinic HEWL crystal under an equilibrium condition. (a) Elementary steps visualized by LCM-DIM, (b) individual F-HEWL molecules (white dots) visualized by TIRF microscopy, (c) a composite image of the images (a) and (c). All images show the same field of view. Dashed rectangles in (a) and (c) show dust particles, which became good markers that ensured the observation of the same field of view. Scale bars represent 5 μm.

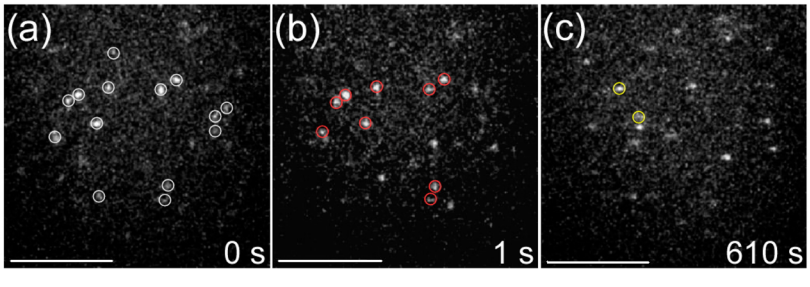

Figure 4. Nonensemble measurements of transient processes of adsorption on a monoclinic HEWL crystal: a typical time-course of F-HEWL molecules appearing on the crystal surface taken 71 min after the molecules were introduced into an observation chamber (t_{ads} = 71 min). Scale bars represent 5 μm. (a) White circles show all the F-HEWL molecules visualized on the crystal surface. Red (b) and yellow (c) circles correspond to the molecules whose positions were not changed for periods longer than 1 and 610 s, respectively.

found in Figure 4a desorbed and then different molecules newly adsorbed at the same locations in Figure 4b (for details, see Supporting Information Figure S2). In other words, the molecules visualized at the same positions show that the molecules were immobilized (adsorbed) for at least 1 s. Hereafter, we define the time interval during which the molecule did not change its position on the crystal surface, as the residence time τ.

Figure 4c shows an image taken 610 s after Figure 4a. Yellow circles indicate the molecules that were not moved between the images in Figure 4a,c: those molecules were adsorbed for at least 610 s ($\tau \geq 610$ s). Note that the number of the molecules of $\tau \geq 610$ s is significantly smaller than that of $\tau \geq 1$ s, showing that many molecules desorbed from the interface during this period. In Figure 4c, molecules not marked by yellow circles newly appeared on the interface after Figure 4a was taken.

dx.doi.org/10.1021/cg501122f | *Cryst. Growth Des.* 2014, 14, 5303−5309

At a given elapsed time after F-HEWL molecules were introduced into the observation chamber, t_{ads} (an elapsed time after the adsorption of F-HEWL molecules started), we measured number density N of F-HEWL molecules whose positions were not changed (within an accuracy of one pixel size) for longer than a residence time τ. Hence, the number density $N(t_{ads}, \geq\tau)$ does not include molecules that were newly adsorbed during the time τ after t_{ads}. The residence time τ was varied from 0.3 s to 20 min. When τ is small, $N(t_{ads}, \geq\tau)$ includes F-HEWL molecules diffusing on the interface. However, adsorbed molecules become the majority of molecules observed, when $\tau \geq 0.47$ s in the case of a tetragonal HEWL crystal.[9] Hence, we assumed that on a monoclinic HEWL crystal, the situation is similar.

We obtained systematic changes in $N(t_{ads}, \geq\tau)$ for various τ, as a function of t_{ads}. The results are shown in Figure 5. In this

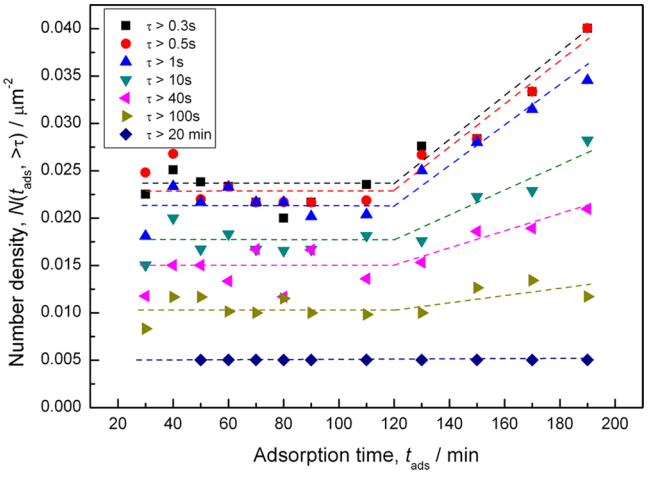

Figure 5. Attachment/detachment processes under an equilibrium condition. Changes in number density $N(t_{ads}, \geq\tau)$ of F-HEWL molecules whose positions were not changed, within an accuracy of one pixel size, for longer than a residence time τ, were plotted as a function of an adsorption time t_{ads}. The residence time τ was varied from 0.3 s to 20 min.

experiment, native HEWL molecules in the solution (1.1 mg/mL) and the monoclinic HEWL crystals (composed of native HEWL molecules) were in equilibrium: therefore, elementary steps did not proceed or recede. In contrast, F-HEWL molecules in the solution (0.1 nM) and the monoclinic HEWL crystals were not in equilibrium, since when $t_{ads} = 0$ min the monoclinic crystals did not contain any F-HEWL molecules on their surfaces. Then, in Figure 5, we observed a very early stage of the adsorption of F-HEWL under the nonequilibrium condition on the crystal surfaces whose steps were not proceeding or receding (a couple of days after the adsorption experiment started, the adsorption appeared to reach equilibrium, although we could not distinguish individual F-HEWL molecules any more because of too many F-HEWL molecules adsorbed on the crystal surfaces).

In Figure 5, it is obvious that an induction period ($t_{ads} \approx 120$ min) existed during which values of $N(t_{ads}, \geq\tau)$ remained almost constant. After the induction time, $N(t_{ads}, \geq\tau)$ increased linearly with the adsorption time t_{ads}. The dashed lines after the induction period show the results of linear fits. As shown in the previous measurement on a tetragonal HEWL crystal (using a 1-μm-thick solution layer),[11] the existence of the induction period was also confirmed on a monoclinic HEWL crystal (using a bulk solution). Hence, we can conclude that the appearance of the induction period is the general phenomenon, irrespective of the kinds of crystals and optical arrangements.

As discussed in the previous study,[11] the existence of the induction period indicates that the adsorption did not proceed through a single-step elementary process. If the adsorption proceeds through a single-step process, the probability by which molecules can overcome an activation energy barrier for adsorption is proportional to the total number of trials, i.e., t_{ads}. Hence, Figure 5 demonstrates that the adsorption proceeded through a series of successive multistep processes. We suppose that dehydration of protein molecules might be a cause for the series of successive multiple processes, although we have no experimental evidence for this supposition at this moment.

Figure 5 also shows that with increasing τ at the same t_{ads}, the value of $N(t_{ads}, \geq\tau)$ significantly and monotonically decreased. This phenomenon was also found on a tetragonal HEWL crystal.[11] The significant decrease in $N(t_{ads}, \geq\tau)$ indicates that stronger adsorption for longer τ is less probable (more difficult) than weaker adsorption for shorter τ. The monotonical decrease in $N(t_{ads}, \geq\tau)$ suggests that during the series of successive multiple processes with increasing τ, the adsorption of molecules becomes gradually stronger: the adsorption proceeds gradually. During the successive multiple processes, if there is a specifically stronger adsorption process at a certain τ than the others, at such τ, $N(t_{ads}, \geq\tau)$ shows a higher value than the others. Hence, from Figure 5, we suggest that the adsorption proceeds gradually. The dehydration hypothesis about the successive multiple processes will also support the gradual adsorption: with a decreasing amount of hydration shells, adsorption will gradually become stronger (although we have no experimental evidence). From the similarities found on both tetragonal and monoclinic HEWL crystals, we conclude that the above-mentioned phenomenon is also a general nature of adsorption.

3.2. Under a Supersaturated Condition. Monoclinic HEWL crystals exhibit a very thin plate shape. Hence, we could visualize individual F-HEWL molecules on a $\{10\bar{1}\}$ face through a monoclinic crystal by TIRF microscopy, using a "bulk solution" (see Supporting Information Figure S1). Here, we emphasize again that the use of a bulk solution enabled us to carry out the fluorescent single-molecule visualization under the growth condition, for the first time. We performed similar measurements of $N(t_{ads}, \geq\tau)$ during the growth of a monoclinic HEWL crystal, using a supersaturated solution (concentration of HEWL: $C = 1.55$ mg/mL, $C - C_e = 0.45$ mg/mL).

Under the growth condition, we analyzed $N(t_{ads}, \geq\tau)$, as schematically shown in Figure 6a. After steps passed the positions where F-HEWL molecules were adsorbed previously, about 90% of F-HEWL molecules disappeared, and about 10% of F-HEWL molecules remained visible after the incorporation into the steps. The incorporation of fluorescent-labeled protein molecules inside HEWL crystals was so far reported in bulk growth experiments.[16−18] But at present, it is unclear whether the disappeared F-HEWL molecules desorbed from the crystal surface or became invisible after being incorporated inside elementary steps. In order to perform the analysis that is equivalent to that in Figure 5, we analyzed only F-HEWL molecules (shown in red) adsorbed on a crystal surface that existed at $\tau = 0$ s, at a certain t_{ads}. We did not analyze F-HEWL molecules (shown in yellow) adsorbed on areas (marked by gray bold bars) newly covered by upstream steps after $\tau = 0$ s, since such molecules had a shorter residence time than the

dx.doi.org/10.1021/cg501122f | Cryst. Growth Des. 2014, 14, 5303−5309

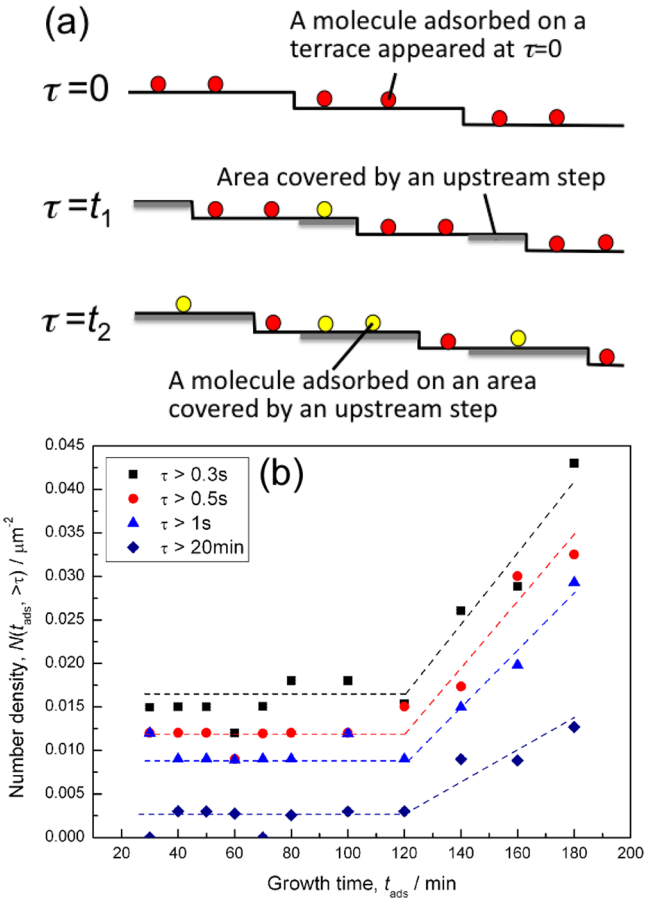

Figure 6. Attachment/detachment processes under a supersaturated (growth) condition. (a) A cross-sectional schematic illustration of the analysis of $N(t_{ads}, \geq\tau)$ under the growth condition at a certain t_{ads}. Red circles show F-HEWL molecules adsorbed on terraces appeared at τ = 0. Yellow circles correspond to F-HEWL molecules adsorbed on areas (marked by gray bold bards) covered by upstream steps after τ = 0. (b) Changes in number density $N(t_{ads}, \geq\tau)$ of F-HEWL molecules whose positions were not changed, within an accuracy of one pixel size, for longer than a residence time τ, as a function of an adsorption time t_{ads}. The residence time τ was varied from 0.3 s to 20 min.

molecules (shown in red) adsorbed on terraces appeared at τ = 0. Hence, $N(t_{ads}, \geq\tau)$ shown in Figure 6b does not include the yellow molecules on the areas colored in gray (Figure 6a), but include only the red molecules.

Results were summarized in Figure 6b. Note that the $N(t_{ads}, \geq\tau)$ vs τ plot also shows the similar induction period (~120 min) under the growth condition, implying that the adsorption proceeded through a series of successive multistep processes also under the growth condition. In addition, Figure 6b also indicates that with increasing τ at the same t_{ads}, the value of $N(t_{ads}, \geq\tau)$ significantly decreased, suggesting that the adsorption of molecules became gradually stronger during a number of trials. These results demonstrate that even under the growth condition, fundamental features of adsorption/desorption processes were the same as those under the equilibrium condition.

In contrast, the $N(t_{ads}, \geq\tau)$ vs τ plot also shows a different feature. The increase in $N(t_{ads}, \geq\tau)$ after the induction period under the growth condition (Figure 6b) is more remarkable than that under the equilibrium condition (Figure 5). The slopes of the straight lines after the induction period correspond to the net adsorption rates.

Then, we plotted the net adsorption rate as a function of a residence time τ. As shown in Figure 7, under both the

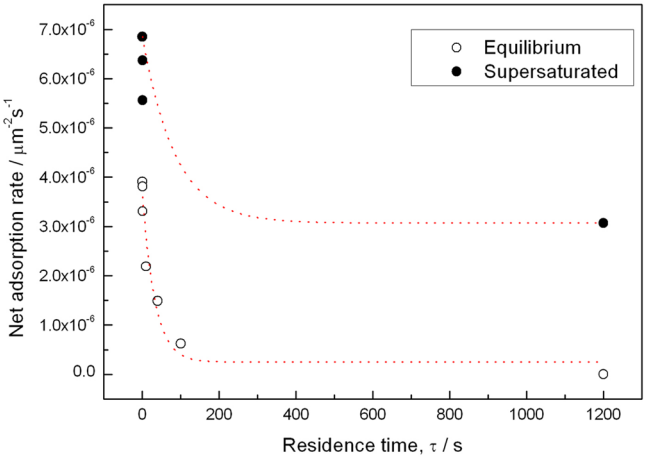

Figure 7. Changes in the net adsorption rates of F-HEWL molecules, which correspond to the slopes of the dashed lines in Figures 5 and 6b after the induction period (~120 min), as a function of a residence time τ. Dashed curves were fitting curves by exponential decay. Open circles: under an equilibrium condition ($C = C_e$ = 1.1 mg/mL), closed circles: under a supersaturated condition (C = 1.55 mg/mL), where C and C_e denote HEWL concentration and solubility, respectively.

equilibrium and supersaturated (growth) conditions, $N(t_{ads}, \geq\tau)$ drastically decreased with increasing τ, and then finally reached almost constant values. Under the equilibrium condition, the net adsorption rate reached ~0 μm^{-2} s^{-1}, showing that the attachment rate was finally equal to the detachment rate under the equilibrium condition. In contrast, under the supersaturated condition, the net adsorption rate reached a positive constant value 3.1 × 10^{-6} μm^{-2} s^{-1}, demonstrating that the attachment rate was significantly faster than the detachment one, and that the attachment and detachment processes finally reached a "steady state". These results clearly indicate that supersaturation significantly enhances the attachment process of individual F-HEWL molecules.

During the attachment and detachment processes, the nature of an adsorption site (i.e., a step or a terrace) is a very important issue. However, as shown in Figure 3, the differential interference contrast of an elementary step has a significantly wide width. Hence, in most of the cases, we could not become confident whether F-HEWL molecules were adsorbed really on steps or on terraces close to steps. Therefore, allow us to make this issue a challenge for the future.

Nevertheless, we found a rare occasion in which an F-HEWL molecule was adsorbed surely on a step. Figure 8 shows such an example found, just by chance, during our preliminary experiment before using 99.99% purity HEWL. In the preliminary experiment, we used 98.5% purity HEWL (6× recrystallized, Seikagaku Co.). Hence, spiral steps (Figure 8) were rougher than those in Figure 3. Figure 8 shows F-HEWL molecules that were adsorbed on a crystal surface for longer than 1 s ($\tau \geq$ 1 s) (marked by black dots, just for visibility). In Figure 8, an F-HEWL molecule (marked by a white circle) followed the advancement of an elementary step (named as step 1). The position of the F-HEWL molecule marked by the

dx.doi.org/10.1021/cg501122f | Cryst. Growth Des. 2014, 14, 5303−5309

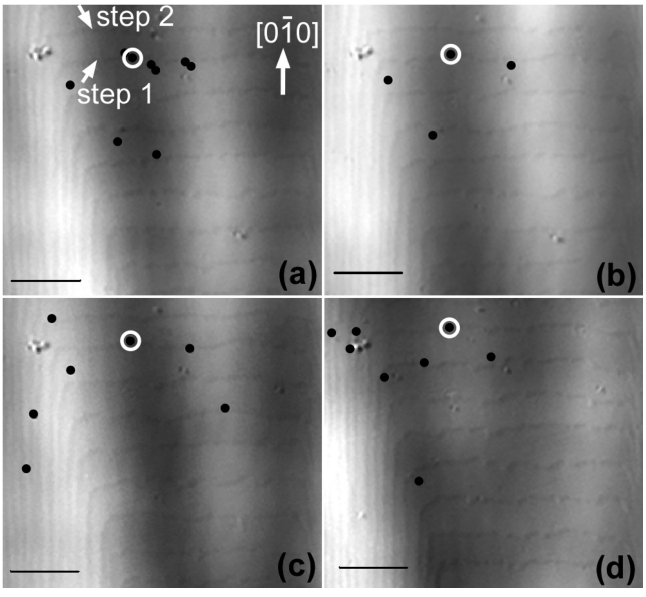

Figure 8. Lateral movement of an F-HEWL molecule adsorbed on an elementary step, under a supersaturated condition, during our preliminary experiment using 98.5% purity HEWL. Since the purity of HEWL was 98.5%, spiral steps were rougher than those in Figure 3. Black dots correspond to F-HEWL molecules with a residence time $\tau \geq 1$ s, just for visibility. White circles show an F-HEWL molecule, which was adsorbed on the step 1 (marked by a white arrowhead), laterally moved following the advancement of the step 1 in the [0$\bar{1}$0] direction. Since the step velocity was 15.3 nm/min, during 82 min the step 1 laterally advanced 1.26 μm, which is shorter than the distance (1.75 μm) between the step 1 and the adjacent step 2. Scale bars represent 5 μm. The image (a) was taken at t_{ads} = 5 min. (a–d) τ = 0, 13, 49, and 82 min, respectively.

white circle continuously changed according to the lateral advancement of the step 1 for 82 min. Hence, we concluded that the F-HEWL molecule was adsorbed surely on the step. Since we found such the molecule during the preliminary experiment, at present it is still unclear whether the appearance of the F-HEWL molecules following the step advancement was due to the roughness of steps caused by impurities. This issue also should be clarified in the near future.

4. CONCLUSIONS

In this study, we observed the attachment/detachment processes of individual F-HEWL molecules on the monoclinic HEWL crystals by TIRF microscopy, utilizing bulk HEWL solutions. We measured the number density $N(t_{ads}, \geq\tau)$ of F-HEWL molecules that were adsorbed on the {10$\bar{1}$} faces longer than the residence time τ, as a function of the adsorption time t_{ads}. Then, we obtained the following key results.

(1) Under the equilibrium condition, the induction period (~120 min) of the attachment/detachment processes existed, as in the case of tetragonal crystals.[11] During this period, $N(t_{ads}, \geq\tau)$ remained constant. After the induction period, $N(t_{ads}, \geq\tau)$ increased with increasing t_{ads}, indicating the existence of successive multistep elementary processes, by which the molecules were gradually immobilized (adsorbed) on the crystal surface.

(2) Under the supersaturated condition, the same induction period (~120 min) also existed. However, after the induction period, supersaturation significantly enhanced the attachment process. When $\tau \geq 20$ min, the attachment and detachment processes reached a steady state: $N(t_{ads}, \geq\tau)$ reached a positive constant value, although under the equilibrium condition the attachment and detachment processes reached an equilibrium state: $N(t_{ads}, \geq\tau)$ reached zero.

(3) In a rare case, the F-HEWL molecule adsorbed on the step laterally moved following the advancement of the growing step.

■ ASSOCIATED CONTENT

Supporting Information

Optical arrangements for the single-molecule visualization by TIRF microscopy, and an F-HEWL molecule visualized at the same position in different frames. This material is available free of charge via the Internet at http://pubs.acs.org.

■ AUTHOR INFORMATION

Corresponding Author

*E-mail: sazaki@lowtem.hokudai.ac.jp. Phone and fax: +81-11-706-6880.

Notes

The authors declare no competing financial interest.

■ ACKNOWLEDGMENTS

G.D. acknowledges the support by National Program on Key Basic Research Project (973 Program) (No. 2011CB710901), and the visiting professorship from Institute of Low Temperature Science, Hokkaido University. G.S. is grateful for the support by Chinese Academy of Sciences visiting professorship for senior international scientists (Grant No. 2013T2J0060). The authors thank Y. Saito and S. Kobayashi (Olympus Engineering Co., Ltd.) for their technical support of LCM-DIM. Funding is from National Program on Key Basic Research Project (973 Program) (No. 2011CB710901); visiting professorship from Institute of Low Temperature Science, Hokkaido University; Chinese Academy of Sciences visiting professorship for senior international scientists (Grant No. 2013T2J0060).

■ ABBREVIATIONS

HEWL, hen egg white lysozyme; F-HEWL, fluorescent-labeled hen egg white lysozyme; AFM, atomic force microscopy; TIRF microscopy, total internal reflection fluorescence microscopy; EM-CCD, electron-multiplying charge-coupled device; LCM-DIM, laser confocal microscopy combined with differential interference contrast microscopy

■ REFERENCES

(1) Moerner, W. E. New directions in single-molecule imaging and analysis. *Proc. Natl. Acad. Sci. U.S.A.* **2007**, *104*, 12596–12602.

(2) Yau, S. T.; Vekilov, P. G. Quasi-planar nucleus structure in apoferritin crystallization. *Nature* **2000**, *406* (6795), 494–497.

(3) Van Driessche, A. E. S.; Otalora, F.; Sazaki, G.; Sleutel, M.; Tsukamoto, K.; Gavira, J. A. Comparison of Different Experimental Techniques for the Measurement of Crystal Growth Kinetics. *Cryst. Growth Des.* **2008**, *8* (12), 4316–4323.

(4) Funatsu, T.; Harada, Y.; Tokunaga, M.; Saito, K.; Yanagida, T. Imaging of Single Fluorescent Molecules and Individual Atp Turnovers by Single Myosin Molecules in Aqueous-Solution. *Nature* **1995**, *374* (6522), 555–559.

(5) Sako, Y.; Uyemura, T. Total internal reflection fluorescence microscopy for single-molecule imaging in living cells. *Cell Struct. Funct.* **2002**, *27* (5), 357–365.

(6) Cognet, L.; Coussen, F.; Choquet, D.; Lounis, B. Fluorescence microscopy of single autofluorescent proteins for cellular biology. *C. R. Phys.* **2002**, *3* (5), 645−656.
(7) Wazawa, T.; Ueda, M. Total internal reflection fluorescence microscopy in single molecule nanobioscience. *Adv. Biochem. Eng. Biotechnol.* **2005**, *95*, 77−106.
(8) Kellermayer, M. S. Z. Visualizing and manipulating individual protein molecules. *Physiol. Meas.* **2005**, *26* (4), R119−R153.
(9) Sazaki, G.; Okada, M.; Matsui, T.; Watanabe, T.; Higuchi, H.; Tsukamoto, K.; Nakajima, K. Single-molecule visualization of diffusion at the solution - Crystal interface. *Cryst. Growth Des.* **2008**, *8* (6), 2024−2031.
(10) Van Driessche, A. E. S.; Sazaki, G.; Dai, G. L.; Otalora, F.; Gavira, J. A.; Matsui, T.; Yoshizaki, I.; Tsukamoto, K.; Nakajima, K. Direct Observation of Adsorption Sites of Protein Impurities and Their Effects on Step Advancement of Protein Crystals. *Cryst. Growth Des.* **2009**, *9* (7), 3062−3071.
(11) Dai, G. L.; Sazaki, G.; Matsui, T.; Tsukamoto, K.; Nakajima, K.; Kang, Q.; Hu, W. R. Gradual Immobilization Processes of Molecules during Transitions from Solute to Solid States. *Cryst. Growth Des.* **2011**, *11* (1), 88−92.
(12) Matsui, T.; Sazaki, G.; Hondoh, H.; Matsuura, Y.; Nakada, T.; Nakajima, K. Impurity effects of lysozyme molecules specifically labeled with a fluorescent reagent on the crystallization of tetragonal and monoclinic lysozyme crystals. *J. Cryst. Growth* **2006**, *293* (2), 415−422.
(13) Hondoh, H.; Sazaki, G.; Miyashita, S.; Durbin, S. D.; Nakajima, K.; Matsuura, Y. Macrobond analysis of the macro- and micro-morphology of monoclinic lysozyme crystal. *Cryst. Growth Des.* **2001**, *1* (4), 327−332.
(14) Sazaki, G.; Matsui, T.; Tsukamoto, K.; Usami, N.; Ujihara, T.; Fujiwara, K.; Nakajima, K. In situ observation of elementary growth steps on the surface of protein crystals by laser confocal microscopy. *J. Cryst. Growth* **2004**, *262* (1−4), 536−542.
(15) Sazaki, G.; Zepeda, S.; Nakatsubo, S.; Yokoyama, E.; Furukawa, Y. Elementary steps at the surface of ice crystals visualized by advanced optical microscopy. *Proc. Natl. Acad. Sci. U.S.A.* **2010**, *107* (46), 19702−19707.
(16) Kurihara, K.; Miyashita, S.; Sazaki, G.; Nakada, T.; Durbin, S. D.; Komatsu, H.; Ohba, T.; Ohki, K. Incorporation of impurity to a tetragonal lysozyme crystal. *J. Cryst. Growth* **1999**, *196* (2−4), 285−290.
(17) Iimura, Y.; Yoshizaki, I.; Nakamura, H.; Yoda, S.; Komatsu, H. Development of fluorescence label and con-focal laser scanning microscopy method for non-destructive local impurity distribution analysis in protein crystals. *Jpn. J. Appl. Phys. Part 1* **2003**, *42* (9A), 5831−5836.
(18) Iimura, Y.; Yoshizaki, I.; Nakamura, H.; Yoda, S.; Komatsu, H. Novel method for measuring the distribution coefficient in protein crystals. *Cryst. Growth Des.* **2005**, *5* (1), 301−305.